Experimentální Analýza Napětí 2010
Experimental Stress Analysis

Experimental Determination of Damping Characteristics of Hybrid Composite Structure

Josef Vacík,[1] Václava Lašová,[2] Radek Kottner,[3] Josef Káňa[4]

Abstract: This paper deals with experimental determination of fundamental natural frequencies and damping ratios of hybrid composite specimens consisting of unidirectional carbon fibre reinforced epoxy composite and rubber. A laser device for measuring displacement was used during the experiments. Records were processed in Matlab. Furthermore, the elastic parameters were verified by comparison of natural frequencies obtained from experiments and numerical simulations.

Keywords: Experimental, Natural frequency, Damping ratio, Hybrid composite, Numerical simulations

1. Introduction

There is a very conservative approach to the application of materials other than steel, cast iron or nodular cast iron in the design of machine tools. The increase of operational speeds of machine tools leads to the demand for light designs of moving bodies with a low moment of inertia, high stiffness and good damping characteristics [1]. Such demands on materials are satisfied by some light-metal alloys, ceramics, *composites* and *hybrid structures*. Hybrid structures consisting of two or more different materials give the advantage of a synergetic effect. For example, a layered composite combined with cork or rubber layers shows better damping ability than the composite alone. Such structures could be successfully used for the supporting structures of machines. To understand dynamic behaviour better, the damping characteristics must be determined. This work deals with experimental determination of damping ratios and fundamental natural frequencies. How the dynamic behaviour of a composite cantilever beam is affected by the integration of rubber layers was investigated during the experiments.

[1] *Ing. Josef Vacík; University of West Bohemia in Pilsen, Faculty of Mechanical Engineering, Department of Machine Design, Univerzitní 8, 306 14 Plzeň, Czech Rep.; jvacik@kks.zcu.cz*
[2] *Doc. Ing. Václava Lašová; Ph.D.; University of West Bohemia in Pilsen, Faculty of Mechanical Engineering, Department of Machine Design, Univerzitní 8, 306 14 Plzeň, Czech Rep.; lasova@kks.zcu.cz*
[3] *Ing. Radek Kottner; Ph.D., University of West Bohemia in Pilsen, Faculty of Applied Science, Department of Mechanics, Univerzitní 8, 306 14 Plzeň, Czech Republic; kottner@kme.zcu.cz*
[4] *Ing. Josef Káňa; University of West Bohemia in Pilsen, Faculty of Applied Sciences, Department of Mechanics, Univerzitní 8, 306 14 Plzeň, Czech Rep.; jkana@kme.zcu.cz*

Experimentální analýza napětí 2010, Petr Šmíd, Pavel Horváth, Miroslav Hrabovský, eds., May 31 - June 3 2010, Velké Losiny, Czech Republic (Palacky University, Olomouc; Olomouc; 2010).

2. Dynamics of damped system

Many parts of machine tools, namely boring bars, headstocks, quills, etc. counter the oscillations. These substructures can be simply represented as a cantilever beam. By focusing on in-plane displacements of the free end, the cantilever beam problem can be treated as a system with a single degree of freedom.

2.1. Equation of motion of damped system with single degree of freedom

By the application of second order Lagrange equations, the motion of discrete linear systems with a single degree of freedom can be described as

$$m\ddot{q} + c\dot{q} + kq = F(t), \tag{1}$$

where $q[m]$, $\dot{q}\left[m \cdot s^{-1}\right]$, $\ddot{q}\left[m \cdot s^{-2}\right]$ is a generalized coordinate and its 1st and 2nd differentiation with respect to time *t*; $F(t)[N]$ is a generalized time-dependent applied force; $m[kg]$ is a mass of the system; $c\left[N \cdot s \cdot m^{-1}\right]$ is a viscous damping constant and $k\left[N \cdot m^{-1}\right]$ is a stiffness constant.

In the case of *free oscillations,* the Eq. (1) can be consequently rewritten to

$$\ddot{q} + 2\zeta\omega_0\dot{q} + \omega_0^{\,2} q = 0, \tag{2}$$

where damping ratio ζ and undamped natural frequency ω_0 are defined as:

$$\zeta = \frac{c}{2\sqrt{mk}}, \tag{3}$$

$$\omega_0 = \sqrt{\frac{k}{m}} \quad \left[rad \cdot s^{-1}\right]. \tag{4}$$

There are three possible states of damped system: *overdamped* ($\zeta > 1$), *critically damped* ($\zeta = 1$) and *underdamped* ($0 < \zeta < 1$) [2].

In the next section, only the underdamped state will be considered. Then, the solution of Eq. (2) representing the displacement of the system can be found in the form:

$$q(t) = Ce^{-\zeta\omega_0 t}\sin(\omega t + \varphi_0), \tag{5}$$

where $C[m]$ is amplitude, $\omega\left[rad \cdot s^{-1}\right]$ is the damped natural frequency of the system and $\varphi_0[rad]$ is phase shift.

The damped natural frequency can be expressed as:

$$\omega = \omega_0\sqrt{1-\zeta^2} = \frac{2\pi}{T}, \tag{6}$$

where $T[s]$ is the period of the waveform (see Fig. 1).

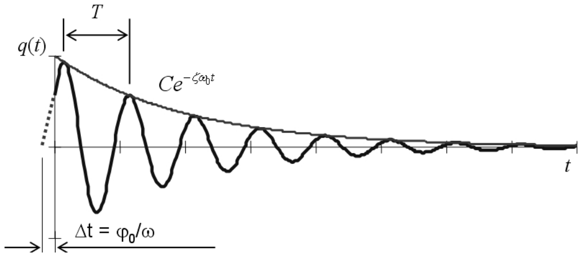

Fig. 1. Response of underdamped harmonic oscillator.

Based on Eq. (5), the *exponential attenuation rate* is then defined:

$$b = \zeta\omega_0 \,. \tag{7}$$

The damping ratio can be determined using the logarithmic decrement δ, which is defined as the natural logarithm of any two peaks:

$$\delta = \frac{1}{n} ln \frac{q_0}{q_n} = \ln e^{\zeta\omega_0 T} = \zeta\omega_0 T = bT = \frac{2\pi\zeta}{\sqrt{1-\zeta^2}} \,, \tag{8}$$

where q_0 is the greater of the two amplitudes and q_n is the amplitude of a peak n periods away. The damping ratio is then found from the logarithmic decrement:

$$\zeta = \frac{\delta}{\sqrt{4\pi^2 + \delta^2}} \,. \tag{9}$$

3. Determination of elastic parameters

A series of experiments was carried out on specimens made of carbon/epoxy lamina (913C-HTS), rubber (65 ShA) and also on the hybrid structure in which the layers were bonded using Loctite 480 glue. Although the rubber exhibits viscoelastic response (Fig. 2), during deformation of less than 10%, it was assumed to show linear elastic behaviour and its mechanical properties were determined using tensile and compressive tests. The specimens were cyclically loaded at 10 mm/min. To avoid the influence of the "Mullin's effect", only the 4th cycles were considered.

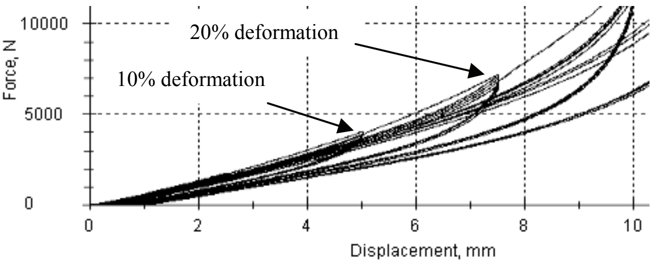

Fig. 2. Viscoelastic behaviour of rubber; Mullin's effect.

The mechanical properties of the entire composite were set with the knowledge of the properties of the fibre and the matrix. The *classical laminate theory* was used with the assumption of transverse isotropic material [3, 4].

Table 1. Mechanical properties

MAT.	PARAMETER		VALUE		NOTE
Rubber	Young's modulus	E_r	10	[MPa]	Isotropic material
	Poisson's ratio	ν_r	0.49		
	Density	ρ_r	1170	[kg.m^{-3}]	
Composite	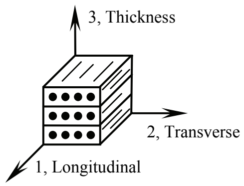	E_1	113.92	[GPa]	Transverse isotropic material
		E_2	5.47	[GPa]	
		G_{12}	2.43	[GPa]	
		ν_{12}	0.34		
		ν_{23}	0.3		
	Density	ρ_c	1560	[kg.m^{-3}]	

4. Verification of elastic parameters

To verify the identified mechanical properties, the modal analyses were computed using Finite Element Method (FEM). Numerical models were created in FEM software MSC Marc 2008r1. The fundamental natural frequencies ($f_{1\mathrm{FEM}}$) were compared with the experimental data. 8-node elements were used.

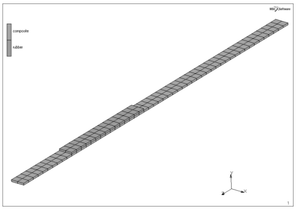

Fig. 3. Preview of one of the numerical models.

5. Experiments

During the experiment, one end of the specimen was clamped and after a slight stroke, the time-dependent displacement *q(t)* of the free end was recorded (Fig. 4) using the *optoNCDT* laser measurement device (Micro-Epsilon co.). The records were processed using the Matlab script to obtain the damping ratio ζ and logarithmic decrement δ (see Fig. 5 for block diagram). First, the value of the exponential attenuation rate was investigated; the parameters of exponential function $y(t) = Ce^{-bt}$ were fitted by interlaying the data peaks using the least square method. Then, according to the theory, the logarithmic decrements – Eq. (8) and damping ratios - Eq. (9) were computed.

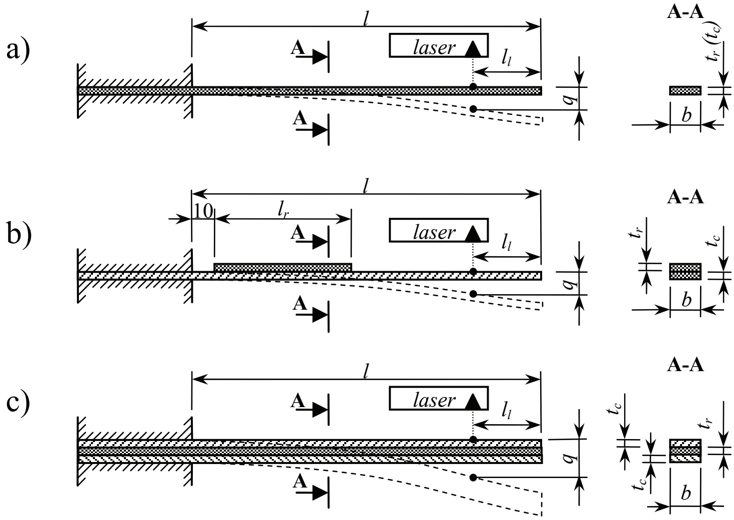

Fig. 4. Arrangement of experiments: a) separate rubber/composite
b) specimen with rubber "patch"
c) hybrid structure specimen.

The dimensions of specimens, the damping ratios and also the comparisons of fundamental natural frequencies are shown in Tables 2 – 8.

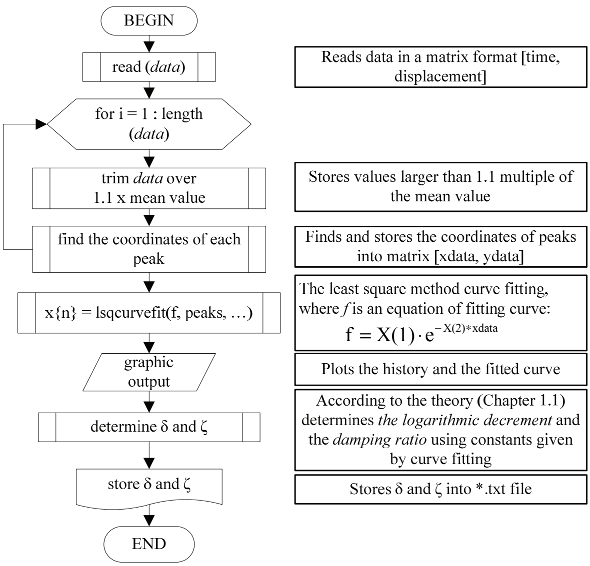

Fig. 5. Block diagram of Matlab script.

Table 2. Specimen №1 – Rubber (Fig. 5a)

l [mm]	l_l [mm]	l_r [mm]	ζ	δ	f_{1EXP} [Hz]	f_{1FEM} [Hz]	freq. error
32.28	1.44	-					
t_r [mm]	t_c [mm]	b[mm]	0.072	0.403	29.8	30.2	+1.3%
3.4	-	6.18					

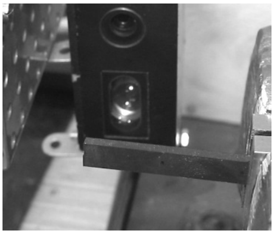

Fig. 6. Specimen №1.

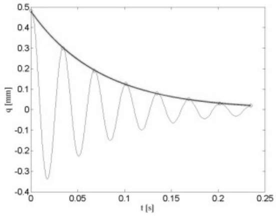

Fig. 7. Damping curve of specimen №1.

Table 3. Specimen №2 – Composite (Fig. 5a)

l [mm]	l_l [mm]	l_r [mm]	ζ	δ	f_{1EXP} [Hz]	f_{1FEM} [Hz]	freq. error
412	82.5	-					
t_r [mm]	t_c [mm]	b[mm]	0.002	0.013	20.4	21.5	+5.4%
-	2.7	19.7					

Fig. 8. Specimen №2.

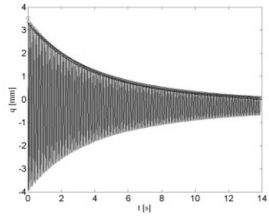

Fig. 9. Damping curve of specimen №2.

Table 4. Specimen №3 – Hybrid structure (Fig. 5b)

l [mm]	l_l [mm]	l_r [mm]	ζ	δ	f_{1EXP} [Hz]	f_{1FEM} [Hz]	freq. error
460	82.5	150					
t_r [mm]	t_c [mm]	b[mm]	0.001	0.008	16.9	17.2	+1.8%
2.4	2.7	19.7					

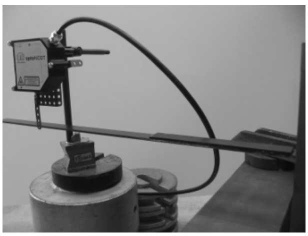

Fig. 10. Specimen №3.

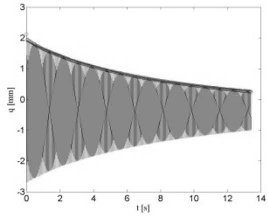

Fig. 11. Damping curve of specimen №3.

Table 5. Specimen №4 – Hybrid structure (Fig. 5b)

l [mm]	l_l [mm]	l_r [mm]	ζ	δ	f_{1EXP} [Hz]	f_{1FEM} [Hz]	freq. error
460	82.5	300					
t_r [mm]	t_c [mm]	b[mm]	0.001	0.008	16.0	16.2	+1.3%
2.4	2.7	19.7					

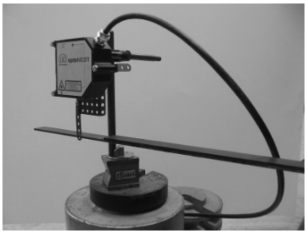

Fig. 12. Specimen №4.

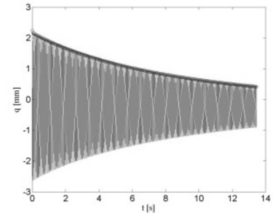

Fig. 13. Damping curve of specimen №4.

Table 6. Specimen №5 – Hybrid structure (Fig. 5b)

l [mm]	l_l [mm]	l_r [mm]	ζ	δ	f_{1EXP} [Hz]	f_{1FEM} [Hz]	freq. error
460	82.5	450					
t_r [mm]	t_c [mm]	b[mm]	0.001	0.009	12.4	13.4	+7.5%
2.4	2.7	19.7					

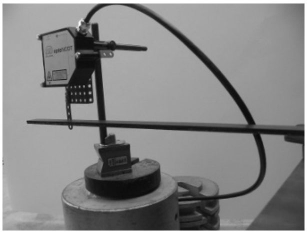

Fig. 14. Specimen №5.

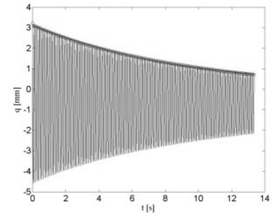

Fig. 15. Damping curve of specimen №5.

Table 7. Specimen №6 – Hybrid structure (Fig. 5c)

l [mm]	l_l [mm]	l_r [mm]	ζ	δ	f_{1EXP} [Hz]	f_{1FEM} [Hz]	freq. error
412	50	-					
t_r [mm]	t_c [mm]	b[mm]	0.034	0.214	35.5	38.6	+8%
2.4	2.7	19.7					

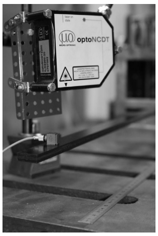

Fig. 16. Specimen №6.

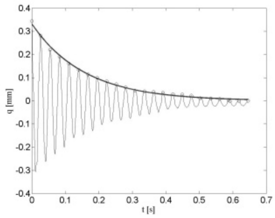

Fig. 17. Damping curve of specimen №6.

Table 8. Specimen №7 – Hybrid structure (Fig. 5c)

l [mm]	l_l [mm]	l_r [mm]	ζ	δ	f_{1EXP} [Hz]	f_{1FEM} [Hz]	freq. error
412	50	-					
t_r [mm]	t_c [mm]	b[mm]	0.043	0.270	44.3	44	-0.7%
2.4	2.7	19.7					

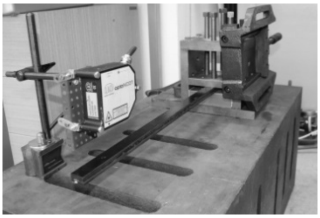

Fig. 18. Specimen №7.

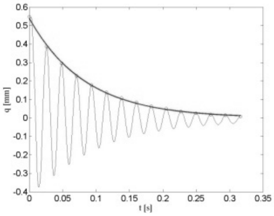

Fig. 19. Damping curve of specimen №7.

6. Conclusion

An experimental determination of damping characteristics was performed on cantilevered specimens and the method of transient response of the system was used. The experiments were performed on the lamina and rubber separately and also on the hybrid structures. The damping ratios were determined using the Matlab script. The elastic parameters were verified by comparing the fundamental natural frequencies obtained both experimentally and from FEM. Although the influences of the adhesive layers, material damping and forces in fixation were not considered in the numerical simulations, a good agreement (less than 10% difference between FE simulations and the experiment) was achieved, which proves that our estimation of material properties was quite accurate. A significant increase in damping is observed for the specimens in which the rubber is placed near the neutral axis, where (according to the Shear formula) shear stress is at a maximum.

In further work, the different structures will be considered. The numerical models created here will be used to optimize the composition of hybrid structures.

Acknowledgements

This paper includes partial results from the Research Project **GA ČR 101/08/0299** and also from the Research Project **GA ČR 101/08/H068**.

References

[1] Lašová V. and Kosnar M., "Využití kompozitních materiálů ve výrobních strojích," in *Proceedings of Mechanika kompozitních materiálů a konstrukcí – MK2*. ZČU Plzeň, Darovanský dvůr u Plzně, March 2009, pp 12-15. ISBN 978-80-7043-782-7.

[2] Zeman V. and Hlaváč Z., *Kmitání mechanických soustav* (ZČU Plzeň, Plzeň, 2004). ISBN 80-7043-337-X.

[3] Laš V., *Mechanika kompozitních materiálů* (ZČU Plzeň, Plzeň, 2004). ISBN 978-80-7043-689-9.

[4] Berthelot J.M., *Composite Materials: Mechanical behaviour and structural analysis* (Springer-Verlag, New York, 1999). ISBN 0-387-98426-7.